Eur. Phys. J. AP (2000)

A Deflated Iterative Solver for Magnetostatic Finite Element Models with Large Differences in Permeability*

H. De Gersem[a] and K. Hameyer

Katholieke Universiteit Leuven, Dep. ESAT, Div. ELEN, Kardinaal Mercierlaan 94, 3001 Leuven - Belgium
phone: 32-16-321020; fax: 32-16-321985; e-mail: Herbert.DeGersem@esat.kuleuven.ac.be

Received: 20 March 2000 / Revised: / Accepted:

Abstract. The presence of materials with a relative large difference in permeability has a harmful influence on the convergence of Krylov subspace iterative solvers. Some slow converging components are not cured by preconditioning and correspond to eigenvectors reflecting the domains with relatively low permeable material. Approximations for those eigenvectors are determined using physical knowledge of the problem. The iterative solution process is split up in a small problem counting for the separated eigenmodes and a full-size problem out of which the slow converging modes are removed. This deflated preconditioned solver is faster converging compared to more common approaches, such as the Incomplete Cholesky Conjugate Gradient method.

Résumé. La présence de matériaux dont les perméabilités sont très différents a une influence néfaste sur la convergence des solveurs itératifs de Krylov. Le préconditionnement ne peut pas améliorer la convergence de certains éléments, dont les vecteurs propres correspondent aux domaines où les matériaux présentent une faible perméabilité. Des approximations pour ces vecteurs propres sont réalisées sur base des caractéristiques physiques du problème. La procédure itérative de résolution est séparée en un problème réduit pour les modes propres de faible convergence, et un modèle complet dont ces mêmes modes sont retirés. Cette méthode converge plus rapidement que les approches conventionnelles, comme la méthode Incomplete Cholesky Conjugate Gradient.

Running title. Deflated Iterative Solver for Magnetostatic Finite Element Models

PACS. 02.60.Cb Numerical simulation; solution of equations - 02.70.Dh Finite-element and Galerkin methods - 84.50.+d Electric motors

1 Introduction

The finite element (FE) procedure translates the continuous field problem into a discrete one represented by a linear system of equations. The solution of the system is usually responsible for the largest part of the simulation time. The simulation of huge models or the application of FE models within iterative design procedures and optimisation is sometimes prohibited by this fact. Recent research deals with the improvement of sparse matrix solvers applied to electromagnetic simulation [1,2]. Krylov subspace solvers are tuned for the particular properties of electromagnetics and multigrid approaches are considered. A large number of simulations however deals with relatively small models in the range of 10^4 degrees of freedom that are sequentially solved for little differences in supply, geometry or material parameters. Usually, a preconditioned Krylov subspace solver, such as e.g. the Incomplete Cholesky (IC) preconditioned Conjugate Gradient (CG) solver is invoked. This paper relates the convergence of CG to the physical properties of the model. The effect of preconditioning is studied. A significant convergence improvement is achieved by supplying the numerical counterpart of the global behaviour of the model to the iterative system solver.

2 Convergence of CG

A Krylov subspace solver extends the base $\begin{bmatrix}\mathbf{v}_1 & \mathbf{v}_2 & \cdots & \mathbf{v}_k\end{bmatrix}$ of the Krylov subspace

$$K_k(\mathbf{r}_0, \mathbf{A}) = \text{span}\left\{\mathbf{r}_0, \mathbf{A}\mathbf{r}_0, \cdots, \mathbf{A}^{k-1}\mathbf{r}_0\right\}, \tag{1}$$

related to the system of n linear equations $\mathbf{A}\mathbf{x} = \mathbf{b}$ and the initial residu $\mathbf{r}_0$, with one new base vector $\mathbf{v}_{k+1}$ at each iteration step. A new iterand $\mathbf{x}_{k+1}$ is searched for within the Krylov subspace. Assuming exact arithmetic, the exact solution is attained at n steps at most. Though, it

* This paper was presented at NUMELEC2000.

[a] e-mail: Herbert.DeGersem@esat.kuleuven.ac.be

is expected that an acceptable approximation for $\mathbf{x}$ is obtained at some $k << n$. In that case, searching for the new iterand corresponds to solving a small-size problem in the Krylov subspace of dimension k. The procedure building the Krylov subspace only requires matrix-vector products and vector updates, making Krylov subspace solvers particularly attractive to solve the sparse systems arising from FE discretisations.

The 2D magnetostatic Poisson equation

$$-\frac{\partial}{\partial x}\left(\nu\frac{\partial A_z}{\partial x}\right)-\frac{\partial}{\partial y}\left(\nu\frac{\partial A_z}{\partial y}\right)=J_z \qquad (2)$$

with A_z the z-component of the magnetic vector potential, ν the reluctivity and J_z the current density, discretised on the domain Ω by finite elements N_i, yields the sparse, symmetric and positive definite system of equations

$$\mathbf{A}\mathbf{x}=\mathbf{b} \qquad (3)$$

with

$$\mathbf{A}_{ij}=\int_{\Omega}\nu\nabla N_i\cdot\nabla N_j d\Omega \qquad (4)$$

and

$$\mathbf{b}_i=\int_{\Omega}J_z N_i d\Omega\,. \qquad (5)$$

The quality of an approximation $\mathbf{x}_k$ for a given k strongly depends upon the properties of the corresponding subspace $K_k(\mathbf{r}_0,\mathbf{A})$. The construction of $K_k(\mathbf{r}_0,\mathbf{A})$ relying upon multiplication with $\mathbf{A}$, reveals that the convergence of Krylov subspace solvers is governed by the eigenvalues and eigenvectors of the system matrix.

The spectrum of $\mathbf{A}$ is real and positive. The spectrum of the system matrix, corresponding to the model problem of Fig. 1, is plotted in Fig. 2a. The CG method is a Krylov subspace method that is naturally related to symmetric, positive definite systems. The convergence of CG applied to (3) is bound by

$$\left\|\mathbf{x}-\mathbf{x}_k\right\|_{\mathbf{A}}\le 2\left\|\mathbf{x}-\mathbf{x}_0\right\|_{\mathbf{A}}\left(\frac{\sqrt{\kappa}-1}{\sqrt{\kappa}+1}\right)^k\,. \qquad (6)$$

The $\mathbf{A}$-norm is defined as $\left\|\mathbf{p}\right\|_{\mathbf{A}}=\sqrt{\mathbf{p}^{\mathrm{T}}\mathbf{A}\mathbf{p}}$. The condition number κ is the ratio between the largest and the smallest eigenvalue [3]. The convergence of CG applied to the model problem is plotted in Fig. 3. The number of iterations and the condition number are collected in Table 1 and Table 2 respectively.

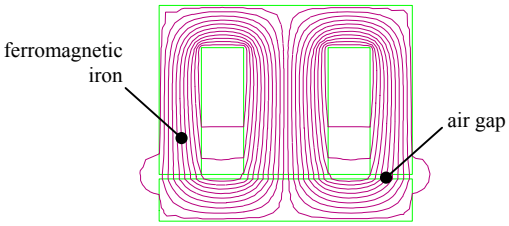

Fig. 1. Magnetic flux plot of an inductor.

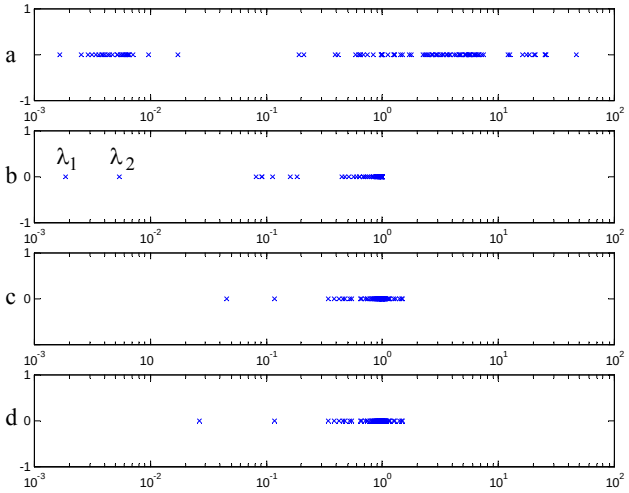

Fig. 2. Spectra of $\mathbf{A}$ (a), $\mathbf{M}^{-1}\mathbf{A}$ (b), $\mathbf{M}^{-1}\mathbf{P}_1^{\mathrm{T}}\mathbf{A}$ (c) and $\mathbf{M}^{-1}\mathbf{P}_2^{\mathrm{T}}\mathbf{A}$ (d).

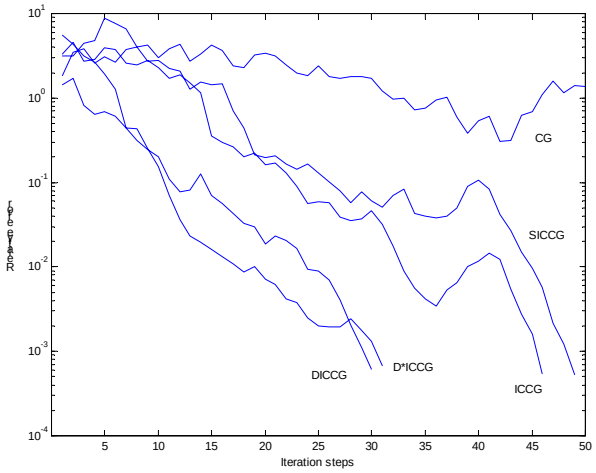

Fig. 3. Convergence histories of CG, ICCG, exact deflated ICCG (DICCG), approximatively deflated ICCG (D*ICCG) and ICCG with an approximative starting solution (SICCG).

Table 1. Number of iterations of CG, ICCG, exact deflated ICCG (DICCG), approximatively deflated ICCG (D*ICCG) and ICCG with an approximative starting solution (SICCG).

number of unknowns	CG	ICCG	DICCG	D*ICCG	SICCG
117	92	22	9	11	18
486	248	46	30	31	49

Table 2. Condition numbers of the system matrices applied to construct the Krylov subspace.

number of unknowns	117	486
CG	2.83e+04	4.02e+04
ICCG	5.37e+02	8.49e+02
DICCG	3.35e+00	4.53e+00
D*ICCG	3.37e+00	4.53e+00
SICCG	5.37e+02	8.49e+02

3 Preconditioning

Better convergence is achieved by applying the Krylov subspace method to the system

$$\mathbf{M}^{-1}\mathbf{A}\mathbf{x} = \mathbf{M}^{-1}\mathbf{b} \tag{7}$$

with $\mathbf{M}$ an appropriate preconditioner [4]. A good preconditioner projects the spectrum of $\mathbf{A}$ to a spectrum of $\mathbf{M}^{-1}\mathbf{A}$ with all eigenvalues in a narrow band around 1, diminishing κ and thus increasing the convergence rate. The preconditioned CG algorithm solving $\mathbf{A}\mathbf{x} = \mathbf{b}$ with starting solution $\mathbf{x}_0$ and preconditioner $\mathbf{M}$ is

Algorithm 1. Preconditioned CG.

$\mathbf{r}_0 = \mathbf{b} - \mathbf{A}\mathbf{x}_0$
$\rho_{-1} = 1;\ \mathbf{p}_0 = 0$
for $k = 1,2,\cdots$
  solve $\mathbf{M}\mathbf{z}_{k-1} = \mathbf{r}_{k-1}$
  $\rho_{k-1} = \mathbf{r}_{k-1}^{\mathrm{T}}\mathbf{z}_{k-1}$
  $\beta_{k-1} = \rho_{k-1}/\rho_{k-2}$
  $\mathbf{p}_k = \mathbf{z}_{k-1} + \beta_{k-1}\mathbf{p}_{k-1}$
  $\mathbf{q}_k = \mathbf{A}\mathbf{p}_k$
  $\alpha_k = \dfrac{\rho_{k-1}}{\mathbf{p}_k^T\mathbf{q}_k}$
  $\mathbf{x}_k = \mathbf{x}_{k-1} + \alpha_k\mathbf{p}_k$
  $\mathbf{r}_k = \mathbf{r}_{k-1} - \alpha_k\mathbf{q}_k$
  stop if convergence
end

As a preconditioner, an Incomplete Cholesky (IC) factorisation is commonly used [5]. The spectrum of $\mathbf{M}^{-1}\mathbf{A}$ is plotted in Fig. 2b. Preconditioning improves the convergence substantially (Fig. 3, Table 1). Two small eigenvalues, λ_1 and λ_2, are left after preconditioning. The iterative solver only reaches the solution when both eigenmodes are incorporated. The convergence history (Fig. 3) reveals that these eigenmodes are difficult to find. The presence of λ_1 and λ_2 has a harmfull influence on the convergence of ICCG. A significant improvement consists of the removal of both eigenmodes out of the system.

4 Origin of the slowly converging eigenmodes

To gain insight into the relation between the physical model and the system spectrum, an eigenvalue decomposition of $\mathbf{M}^{-1}\mathbf{A}$ is performed. The two eigenvectors corresponding to λ_1 and λ_2 are plotted in Fig. 4. $\mathbf{u}_1$ and $\mathbf{u}_2$ correspond to flux patterns that are expected from the physical point of view: they reveal the major behaviour of the flux because of the large permeability of the iron parts in the model (Fig. 5). As a consequence, the slow converging eigenmodes are related to the presence of large differences in permeability in the model. The two small eigenvalues appearing in the spectrum are related to the two existing degrees of freedom for the global magnetic flux in the iron parts of the model.

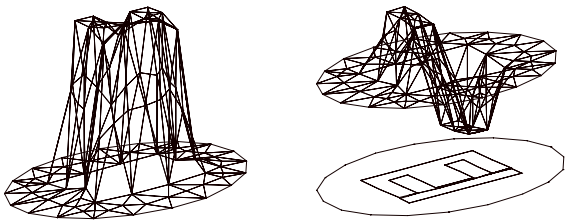

Fig. 4. Eigenvectors $\mathbf{u}_1$ and $\mathbf{u}_2$ of $\mathbf{M}^{-1}\mathbf{A}$ corresponding to λ_1 and λ_2.

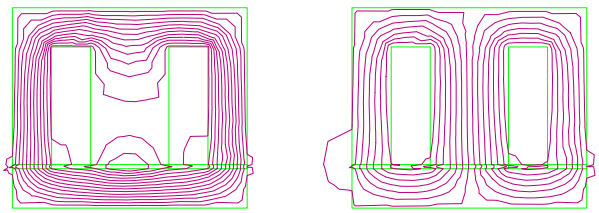

Fig. 5. Flux patterns corresponding to $\mathbf{u}_1$ and $\mathbf{u}_2$.

5 Deflated ICCG

The Krylov subspace incorporates the eigenmodes $(\lambda_1, \mathbf{u}_1)$ and $(\lambda_2, \mathbf{u}_2)$ only after a considerable number of iteration steps. This is because $\mathbf{u}_1$ and $\mathbf{u}_2$ correspond to small eigenvalues and are as a consequence not favoured by the construction procedure for $K_k\left(\mathbf{r}_0, \mathbf{M}^{-1}\mathbf{A}\right)$, relying upon multiplication with $\mathbf{M}^{-1}\mathbf{A}$. To overcome this effect, either the Krylov space can be

explicitly enriched by $\mathbf{u}_1$ and $\mathbf{u}_2$ or the eigenmodes related to $\mathbf{u}_1$ and $\mathbf{u}_2$ can be removed out of the linear system of equations [6]. The latter approach is proposed here.

Consider the partial eigenspace U with as a base, the orthonormal set $\mathbf{U}=[\mathbf{u}_1 \quad \mathbf{u}_2]$ associated with the eigenmodes $(\lambda_1,\mathbf{u}_1)$ and $(\lambda_2,\mathbf{u}_2)$. Define the operator

$$\mathbf{P}_1 = \mathbf{I} - \mathbf{U}\mathbf{E}_1^{-1}(\mathbf{A}\mathbf{U})^{\mathrm{T}} \tag{8}$$

with $\mathbf{E}_1 = (\mathbf{A}\mathbf{U})^{\mathrm{T}}\mathbf{U}$. $\mathbf{P}_1$ is a projector ($\mathbf{P}_1^2 = \mathbf{P}_1$) and commutates with $\mathbf{A}$ as $\mathbf{P}_1^{\mathrm{T}}\mathbf{A} = \mathbf{A}\mathbf{P}_1$ [3]. $\mathbf{P}_1$ projects all vectors $\mathbf{x}$ upon $\mathbf{P}_1\mathbf{x} \in U$ with U the space spanned by $\mathbf{u}_1$ and $\mathbf{u}_2$. $\mathbf{E}_1$ is a low dimensional matrix which inverse is computed in advance. $\mathbf{P}_1$ defines a decomposition of the n-dimensional space $\Re^n$ with respect to the $\mathbf{A}$-inner product, into two orthogonal spaces U and $U^{\perp}$:

$$\Re^n = U \oplus U^{\perp}. \tag{9}$$

The solution $\mathbf{x}$ is split up in two components:

$$\mathbf{x} = (\mathbf{I}-\mathbf{P}_1)\mathbf{x} + \mathbf{P}_1\mathbf{x}. \tag{10}$$

$(\mathbf{I}-\mathbf{P}_1)\mathbf{x}$ is the component of the solution contained in the low dimensional space U spanned by $\mathbf{U}$. $(\mathbf{I}-\mathbf{P}_1)\mathbf{x}$ is computed by

$$(\mathbf{I}-\mathbf{P}_1)\mathbf{x} = \mathbf{U}\mathbf{E}_1^{-1}\mathbf{U}^{\mathrm{T}}\mathbf{b}. \tag{11}$$

This component represents the participation of $\mathbf{u}_1$ and $\mathbf{u}_2$ to the solution of the model. The second component $\mathbf{P}_1\mathbf{x}$ is perpendicular to U in the $\mathbf{A}$-inner product. $\mathbf{x}$ is solved from the deflated system

$$\mathbf{M}^{-1}\mathbf{P}_1^{\mathrm{T}}\mathbf{A}\mathbf{x} = \mathbf{M}^{-1}\mathbf{P}_1^{\mathrm{T}}\mathbf{b} \tag{12}$$

obtained by projecting (7) upon $U^{\perp}$. $U^{\perp}$ does not contain the eigenvectors $\mathbf{u}_1$ and $\mathbf{u}_2$. As a consequence, applying CG to (12) is more efficient compared to (7) [7]. λ_1 and λ_2 are projected upon zeros in the spectrum of $\mathbf{M}^{-1}\mathbf{P}_1^{\mathrm{T}}\mathbf{A}$ (Fig. 2c), indicating the rank deficiency of the projected system. CG is still applicable if the righthandside is contained in the range of the singular system matrix, as is here [8]. In that case, the eigenmodes $(\lambda_1,\mathbf{u}_1)$ and $(\lambda_2,\mathbf{u}_2)$ do not participate in the Krylov process. However, the solution contains an unknown component in U, the null-space of $\mathbf{M}^{-1}\mathbf{P}_1^{\mathrm{T}}\mathbf{A}$. Therefore, the solution $\mathbf{x}$ has to be restricted properly to $\mathbf{P}_1\mathbf{x}$ [8]. The deflated algorithm is derived from the preconditioned CG algorithm by applying deflation by $\mathbf{P}_1^{\mathrm{T}}$ to the matrix-vector product and proper projection by $\mathbf{P}_1$ after the iteration loop.

Algorithm 2. Preconditioned CG, deflated by projector $\mathbf{P}$.

$\mathbf{r}_0 = \mathbf{P}^{\mathrm{T}}(\mathbf{b} - \mathbf{A}\mathbf{x}_0)$
$\rho_{-1} = 1;\ \mathbf{p}_0 = 0$
for $k = 1,2,\cdots$
  solve $\mathbf{M}\mathbf{z}_{k-1} = \mathbf{r}_{k-1}$
  $\rho_{k-1} = \mathbf{r}_{k-1}^{\mathrm{T}}\mathbf{z}_{k-1}$
  $\beta_{k-1} = \rho_{k-1}/\rho_{k-2}$
  $\mathbf{p}_k = \mathbf{z}_{k-1} + \beta_{k-1}\mathbf{p}_{k-1}$
  $\mathbf{q}_k = \mathbf{P}^{\mathrm{T}}\mathbf{A}\mathbf{p}_k$
  $\alpha_k = \dfrac{\rho_{k-1}}{\mathbf{p}_k^T\mathbf{q}_k}$
  $\mathbf{x}_k = \mathbf{x}_{k-1} + \alpha_k\mathbf{p}_k$
  $\mathbf{r}_k = \mathbf{r}_{k-1} - \alpha_k\mathbf{q}_k$
  stop if convergence
end
$\mathbf{x} = \mathbf{P}\mathbf{x}_k + \mathbf{U}\mathbf{E}^{-1}\mathbf{U}^{\mathrm{T}}\mathbf{b}$

The deflated version of the ICCG solver (DICCG) provides an extra gain of convergence (Fig. 3, Table 1, Table 2). The application of $\mathbf{P}_1^{\mathrm{T}}$ introduces a few vector-vector updates per iteration step.

6 Approximative eigenvectors

The exact determination of the considered eigenvectors would cost more work than the solution of (7) itself. Section 4 indicates that approximations for these vectors can easily be obtained on a heuristic basis. Approximative eigenvectors $\mathbf{W}=[\mathbf{w}_1 \quad \mathbf{w}_2]$ are constructed assuming the magnetic flux to be homogeneously distributed in the flux tubes formed by the high permeable iron parts and the air gaps of the model. The flux leakage in the coil and outside the iron core is neglected. The flux patterns are much alike those of Fig. 5. The projector using the approximative eigenvectors $\mathbf{w}_1$ and $\mathbf{w}_2$ is

$$\mathbf{P}_2 = \mathbf{I} - \mathbf{W}\mathbf{E}_2^{-1}(\mathbf{A}\mathbf{W})^{\mathrm{T}} \tag{13}$$

with $\mathbf{E}_2 = (\mathbf{A}\mathbf{W})^{\mathrm{T}}\mathbf{W}$ [7]. Also $\mathbf{P}_2$ is a projector ($\mathbf{P}_2^2 = \mathbf{P}_2$) and commutates with $\mathbf{A}$ ($\mathbf{P}_2^{\mathrm{T}}\mathbf{A} = \mathbf{A}\mathbf{P}_2$). $\mathbf{P}_2$ projects all vectors $\mathbf{x}$ upon $\mathbf{P}_2\mathbf{x} \in W$ with W the space spanned by $\mathbf{w}_1$ and $\mathbf{w}_2$.

The application of a projector $\mathbf{P}$ with m deflating vectors mainly involves m inner products and m vector updates. The computation in the low-dimensional approximative eigenspace (the factorisation of $\mathbf{E}$ and the backsubstitutions) is negligible if m is much lower than the size of the matrix system. If the original system matrix has a bandwidth comparable to m, the application of $\mathbf{P}$ may be too expensive. As only the space W is of importance, the cost of $\mathbf{P}_2$ can be further reduced by replacing $\mathbf{w}_1$ and $\mathbf{w}_2$ by base vectors $\mathbf{q}_1$ and $\mathbf{q}_2$ of W with a more local support (Fig. 6) [7]. The two small eigenvalues correspond to the two independent loop fluxes that can be considered in the iron parts of the model (Fig. 7). The algebraic sparsity of $\mathbf{Q} = [\mathbf{q}_1 \quad \mathbf{q}_2]$ enables an efficient application of the projector

$$\mathbf{P}_3 = \mathbf{I} - \mathbf{Q}\mathbf{E}_3^{-1}(\mathbf{A}\mathbf{Q})^{\mathrm{T}} \tag{14}$$

with $\mathbf{E}_3 = (\mathbf{A}\mathbf{Q})^{\mathrm{T}}\mathbf{Q}$ [7].

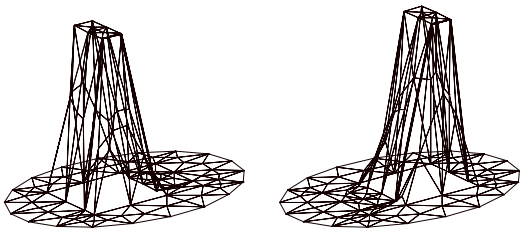

Fig. 6. Base vectors $\mathbf{q}_1$ and $\mathbf{q}_2$ of the approximative eigenspace W corresponding to the small eigenvalues of $\mathbf{M}^{-1}\mathbf{A}$.

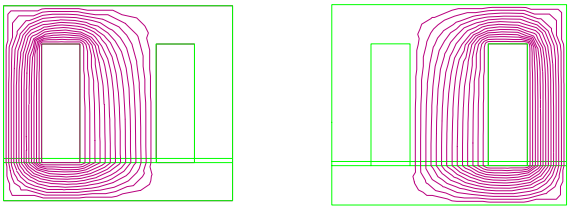

Fig. 7. Flux patterns corresponding to the base vectors $\mathbf{q}_1$ and $\mathbf{q}_2$.

The performance of the approximately deflated method depends on the accuracy of the approximative eigenspace with respect to the eigenspace corresponding to the slow converging eigenmodes. The numerical tests (D*ICCG in Fig. 2, Table 1), however, show that a rough approximation is sufficient to obtain a significant convergence improvement. The approximately deflated version of the ICCG solver provides an extra gain of convergence to which the extra work introduced by $\mathbf{P}_2$ in the algorithm is negligible.

In the design practice, the small-sized modellisation, such as e.g. a magnetic equivalent circuit, is always carried out before proceeding to a FE model. A common link between both models consists of supplying the solution of the rough model as a starting solution for the iterative solver within the FE simulation. This approach yields a little speed-up (Fig. 3, Table 1, Table 2) but is less effective when compared to deflation as it does not deactivate the slow converging modes in the construction procedure of the Krylov subspace. The deflated version of ICCG, presented here, recycles the rough information inside the Krylov subspace itself, curing the bad convergence due to high differences in permeability.

7 Application

The deflated ICCG solver is applied to simulate the zero-load operation of an induction machine. The FE model suffers from the large number of slots and cooling channels in the geometry. From a magnetic point of view, they can not be neglected as they are responsible for a significant decrease in permeability of the stator and rotor yokes. They introduce large jumps in material coefficients and as a consequence, slowly converging eigenmodes in the system matrix.

A magnetic equivalent circuit model is appropriate for a fast simulation of this device. A geometric algorithm determines the reluctances of the magnetic paths formed by the stator and the rotor iron and the air gap. Flux leakage in the slots and the cooling channels is neglected. The same algorithm can be applied to construct the vectors attached to the FE mesh corresponding to the flux distributions of the independent loops in the circuit. Each loop consists of two stator teeth, a few rotor teeth, a part of the stator and the rotor yoke and two passes through the air gap. The FE vectors have a relatively local support and enable the construction of an efficient projector $\mathbf{P}_2$. Iteration counts of the deflated ICCG algorithm are compared to those of CG and ICCG in Table 3. For this example, deflation diminishes the solution time by a factor of 7. The application of the circuit solution as a starting solution for CG only brings a negligible speed-up of the system solution.

A practical disadvantage of this technique is the strong liaison between the modelling part and the system solving part in the software. Usually, the system solution is considered as a black-box operation. The Krylov subspace forms the deepest level on which a solution is determined. Here, the modelling information is propagated from the pre-processing routines up to the Krylov subspace algorithms. The considerable speed-up provided by deflation, however, justifies all efforts to recycle heuristic modelling information in the system solution.

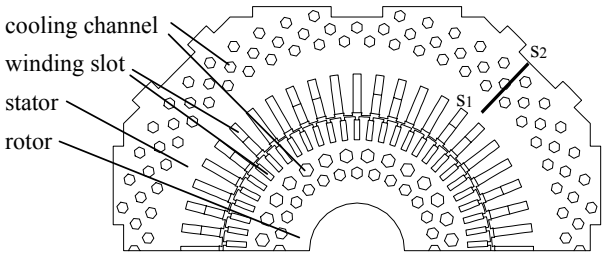

Fig. 8. Geometry of the four-pole induction motor.

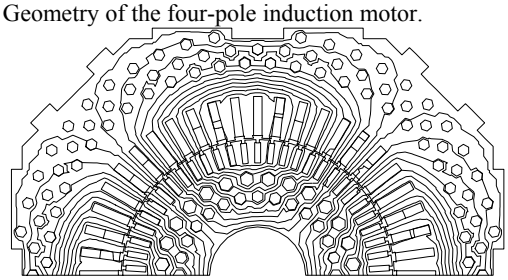

Fig. 9. Magnetic flux lines in the induction motor.

8 Conclusions

Large discontinuous variations of the permeability in magnetic models give raise to bad convergence properties of the IC preconditioned CG iterative method applied to solve the linear system of equations. The eigenvectors corresponding to the slowly converging eigenmodes establish flux patterns that are easily approximated on heuristic grounds. An eigenspace approximating the space spanned by these eigenmodes is supplied to the deflated version of the Krylov subspace solver and yields a considerable improvement of the convergence of ICCG. The approach, presented here, indicates a powerful way to benefit from rough models to diminish the simulation times of finite element models.

Table 3. Comparion of the convergences of CG, IC preconditioned CG and ICCG deflated by approximative eigenvectors.

Solver	Number of iteration steps
CG	1753
ICCG	383
D*ICCG	62
SICCG	372

Acknowledgement

The authors are grateful to the Belgian “Fonds voor Wetenschappelijk Onderzoek - Vlaanderen” for its financial support of this work (project G.0427) and the Belgian Ministry of Scientific Research for granting the IUAP No. P4/20 on Coupled Problems in Electromagnetic Systems. The research Council of the K.U.Leuven supports the basic numerical research.

References

[1] M. Clemens, R. Schuhmann, U. van Rienen, T. Weiland, ACES Journal on Applied Mathematics: meeting the challenges presented by computational electromagnetics 11, 1 (1996).
[2] I. Tsukerman, A. Plaks, IEEE Trans. on Magn. 35, 3 (1999).
[3] Y. Saad, *Iterative Methods for Sparse Linear Systems* (PWS Publishing Company, Boston, 1996).
[4] R. Barrett, M. Berry, T. Chan, J. Demmel, J. Donato, J. Dongarra, V. Eijkhout, R. Pozo, C. Romine, H. Van der Vorst, *Templates for the solution of linear systems: building blocks for iterative methods* (SIAM, Philadelphia, 1994).
[5] K. Fujiwara, T. Nakata, H. Fusayasu, IEEE Trans. on Magn. 29, 2 (1993).
[6] A. Chapman, Y. Saad, University of Minnesota Report No. umsi-95-181, 1995 (unpublished).
[7] C. Vuik, A. Segal, J.A. Meijerink, J. Comp. Phys. 152 (1999).
[8] E.F. Kaasschieter, J. Compl. Appl. Math. 24 (1988).